Solar Energy Materials & Solar Cells 104 (2012) 152–158

Contents lists available at SciVerse ScienceDirect

Solar Energy Materials & Solar Cells

journal homepage: www.elsevier.com/locate/solmat

Copper–indium–gallium–selenide (CIGS) solar cells with localized back contacts for achieving high performance

Marko Nerat *

Jožef Stefan Institute (JSI), Jamova 39, SI–1000 Ljubljana, Slovenia

ARTICLE INFO

Article history:
Received 24 October 2011
Received in revised form
9 May 2012
Accepted 16 May 2012
Available online 7 June 2012

Keywords:
CIGS solar cells
Localized back contacts
Modeling in 2D

ABSTRACT

Thin-film, polycrystalline, CIGS solar cells with localized and whole back contacts were modeled and simulated in two dimensions (2D) in order to investigate their potential for achieving high performance. The simulation results show that the short-circuit current density (J_{sc}) of the CIGS cells with localized back contacts increases with a decreasing contacted area due to the decreased cumulative surface recombination rate at the back side of the CIGS layer. The conversion efficiency (η) of these thin-film, CIGS cells can be increased by 15% relatively compared to CIGS cells with traditional whole back contacts if the surface-recombination velocity of the electrons and the holes ($s_{n/p}$) between two adjacent fingers of the back contact is zero and the density of the acceptor defect states (N_{tA}) inside the CIGS layer is low ($N_{tA} < 10^{13}$ cm^{-3}). The polycrystalline properties of the CIGS were modeled by setting vertical grain boundaries (GBs) within the CIGS absorbent layer. The simulation results show that a valence-band offset (*VBO*) above 0.2 eV at the GBs increases the J_{sc}, but it also significantly reduces the fill factor (FF) of the CIGS cells with localized back contacts. The results show that the efficiency of the CIGS cells with localized back contacts can be increased by 7% relatively if the density of the acceptor defect states at the GBs ($N_{tA,GB}$) equals 10^{17} cm^{-3}. In contrast, the efficiency of the CIGS cells with localized back contacts can be increased by only 1% relatively at the same $N_{tA,GB}$ if the *VBO* is 0.5 eV.

1. Introduction

CIGS solar cells have the highest conversion efficiency (η) of thin-film cells. The current world-record efficiency for a single-junction, thin-film, polycrystalline, CIGS cell exceeds 20% under standard test conditions (STCs) [1]. However, this efficiency could be increased in the future since the current record efficiency represents approximately two-thirds of the thermodynamic limit for a single-junction cell [2,3]. The efficiency of CIGS cells can be increased by applying localized back contacts. This concept has shown that the efficiency of crystalline Si solar cells can be increased [4]. Several studies have focused on numerical simulations and the optimization of Si solar cells with localized contacts [5–7]. The contacted fraction, defined as the metal-semiconductor contact area divided by the total cell area, emerges as the key parameter to be optimized [5]. Schöfthaler et al. presented a study that takes into account the electronic properties of the inhomogeneous back surface, partially metal covered and partially passivated [6]. Aberle et al. analyzed the different approaches published to date. In this article there is a discussion about the validity of those approaches, claiming that the two-dimensional (2-D) analysis they performed fulfills, reasonably well, the simulation requirements of the high-efficiency, Si PERL, solar cells fabricated at the UNSW [7].

There are several papers about the numerical modeling and simulations of CIGS solar cells in two dimensions (2D) [8–11]. Some of these studies also consider the grain boundaries (GBs) within the CIGS absorbent layer. However, numerical modeling and simulations of CIGS solar cells with localized back contacts have not been reported so far. The purpose of this study is to model these cells in order to study their performance by means of simulation results. The main motivation was to verify whether a reduced surface-recombination rate between two adjacent, localized, back contacts could possibly increase the efficiency of the CIGS cells, like with the Si PERL cells.

The back contact for a CIGS cell is commonly made of a thin molybdenum (Mo) layer on a substrate. There are several processes that can be used to form a localized back contact for a CIGS cell: laser scribing [12], photolithography followed by chemical etching [13], or Mo ink printing [14]. The laser ablation of metals [12] and transparent materials with ultra-short UV and IR pulses, respectively, has been demonstrated to yield well-defined microstructures [15,16]. The structuring of solar cells with IR and UV laser sources has been studied extensively [17–20]. An important parameter for the modeling of a CIGS cell with a localized back contact is a minimal width between the fingers of the back

* Tel.: +386 1 477 3240; fax: +386 1 477 3994.
E-mail address: Marko.Nerat@ijs.si

0927-0248/$ - see front matter © 2012 Elsevier B.V. All rights reserved.
http://dx.doi.org/10.1016/j.solmat.2012.05.020

contact, which is limited by the laser-beam diameter [21]. Therefore, a minimum cutting width of 2 μm is considered in the modeling of the CIGS structures.

The CIGS solar cells are modeled and simulated in 2D with an ASPIN2 electrical simulator [22]. The code of this simulator is written in the C#/C++ programming language and it implements the standard drift-diffusion (DD) model [23] for semiconductors in 1D and 2D, including some extensions for solving hetero-junction devices.

2. Methods

Fig. 1 shows cross-section profiles of the modeled and simulated CIGS solar cells. These structures consist of seven layers on a substrate, in the following order: Mo back contact, CIGS/CIGS ordinary vacancy compound (OVC) absorber, CdS buffer, i-ZnO window, ZnO:Al window/front contact and MgF_2 anti-reflective layer. The thicknesses of these layers are also labeled. Most of the important electrical parameters for the simulations in 2D are summarized in Table 1 [8–10,24–29].

The surface-recombination velocity ($s_{n/p}$) at the CIGS/Mo interface is equal to the thermal velocity of the electrons/holes ($v_{n/p}$) [8,24]. The $s_{n/p}$ at the CIGS/substrate interface (between the fingers of the back contact) is assumed to be zero, since an almost ideal surface passivation ($s_{n/p} \approx 0$ cm s^{-1}) of the CIGS using atomic-layer-deposited Al_2O_3 can be achieved [30]. The MgF_2 layer with a thickness of 100 nm is used as an anti-reflective coating. This layer serves only to reduce the reflectance and increases the output performance of the CIGS cell since more light can be absorbed. The Mo and MgF_2 layers are not considered in the electrical simulations, but only in the optical simulations in 1D with the optical simulator Sun*Shine* [31] and they are excluded from the simulation domain (SD). The CIGS cell is simulated under AM1.5 spectrum irradiance with a power density of 100 mW cm^{-2} and a temperature of 25 °C.

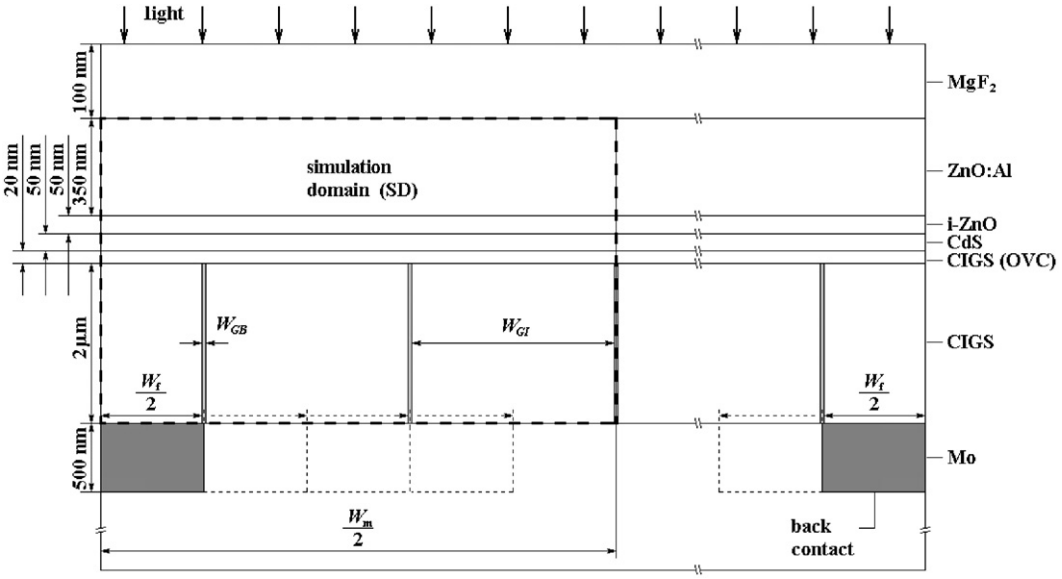

Fig. 1. Modeled and simulated CIGS solar cells with localized back contact. The width of the finger and module is denoted with W_f and W_m, respectively. The structure with a whole back contact is obtained when W_f equals W_m. The vertical grain boundaries (GBs) inside the CIGS are also modeled: the widths of the GB and the grain are denoted by W_{GB} and W_{GI} (W_{GB}=25 nm, W_{GI}=2 μm).

Table 1
Input parameters for simulations.

	ZnO:Al	i-ZnO	CdS	CIGS (OVC)	CIGS
T (K)	298	298	298	298	298
t (nm)	350	50	50	20	2000
N_D (cm^{-3})	1.0×10^{18}	1.0×10^{16}	2.0×10^{17}	–	–
N_A (cm^{-3})	–	–	–	2.0×10^{16}	2.0×10^{16}
E_g (eV)	3.30	3.10	2.40	1.35	1.15
E_χ (eV)	4.5	4.5	4.3	4.5	4.5
m_n / m_0	0.2	0.2	0.2	0.2	0.2
m_p / m_0	0.8	0.8	0.8	0.8	0.8
ε / ε_0	9.0	9.0	10.0	13.6	13.6
μ_n ($cm^2\,V^{-1}\,s^{-1}$)	100	100	40	40	40
μ_p ($cm^2\,V^{-1}\,s^{-1}$)	25	25	10	10	10
N_{tD} (cm^{-3})	1.0×10^{14}	1.0×10^{14}	1.0×10^{17}	1.0×10^{12}	1.0×10^{12}
N_{tA} (cm^{-3})	1.0×10^{12}	1.0×10^{12}	1.0×10^{12}	1.0×10^{14}	1.0×10^{12}
E_{tD} (eV)	E_v+1.65	E_v+1.55	E_v+1.20	E_v+1.00	E_v+0.80
E_{tA} (eV)	E_c−1.65	E_c−1.55	E_c−1.20	E_c−0.80	E_c−0.80
σ_{nD} (cm^2)	1.0×10^{-13}	1.0×10^{-13}	1.0×10^{-15}	5.0×10^{-13}	5.0×10^{-13}
σ_{pD} (cm^2)	1.0×10^{-15}	1.0×10^{-15}	1.0×10^{-17}	1.0×10^{-15}	1.0×10^{-15}
σ_{nA} (cm^2)	1.0×10^{-17}	1.0×10^{-17}	1.0×10^{-15}	5.0×10^{-15}	5.0×10^{-15}
σ_{pA} (cm^2)	1.0×10^{-15}	1.0×10^{-15}	1.0×10^{-13}	1.0×10^{-14}	1.0×10^{-14}
v_n (cm s^{-1})	6×10^6	6×10^6	6×10^6	6×10^6	6×10^6
v_p (cm s^{-1})	3×10^6	3×10^6	3×10^6	3×10^6	3×10^6